Int. J. Electrochem. Sci., 7 **(2012)** 8688 - 8701

International Journal of
ELECTROCHEMICAL
SCIENCE
www.electrochemsci.org

Electrochemical Study of Oxyanions Effect on Galvanic Corrosion Inhibition

I. Carrillo[1], *B. Valdez*[1,*], *R. Zlatev*[1], *M. Stoytcheva*[1], *M. Carrillo*[1], *R. Bäßler*[2]

[1] Corrosion laboratory, Engineering Institute, Autonomous University of Baja California, Mexicali, Mexico
[2] Federal Institute for Materials Research and Testing, Berlin, Germany
[*]E-mail: benval@uabc.edu.mx

Received: 19 July 2012 / *Accepted:* 10 August 2012 / *Published:* 1 September 2012

A comparative study of how oxyanions, e.g. molybdates, in combination with silicate, nitrite and phosphate prevent and control the galvanic corrosion was carried out in order to evaluate their effectiveness and to investigate the corrosion inhibition mechanism. Specimens of copper (Cu) and carbon steel (CS) were studied by electrochemical impedance spectroscopy (EIS) under coupled and uncoupled conditions in inhibited soft water. Stagnant and circulating flow solutions at different temperatures were also employed. The results show that the diffusion of species is affected by the hydrodynamic conditions and temperature. An inhibition mechanism was proposed through equivalent circuits. The calculated nominal polarization resistance (R_{po}) indicates different levels of inhibition performance when Cu, CS and Cu-CS galvanic couple were separately evaluated. We show that molybdate anions in combination with nitrite, silicate and phosphate form deposits with an oxide/hydroxide layer in anodic sites where the metal dissolves. Since the inhibition process begins with adsorption at the metal–solution interface, protection performance depends on the properties of the complex formed by the inhibitor ions and metals.

Keywords: oxyanions, molybdate, galvanic couple, corrosion inhibition

1. INTRODUCTION

Many oxyacid salts such chromates, molybdates, nitrites, phosphates, borates and tungstates have been employed in previous research because of their inhibitory properties against corrosion [1–9]. Since chromate toxicity is a limiting factor in the use of chromate as an inhibitor, molybdate-based corrosion inhibitors represent a good alternative because of their very low levels of toxicity [9, 10]. Molybdates are known for their effectiveness as corrosion inhibitors, which allows them to protect CS,

steel alloys, aluminum and other metals [3, 4, 6, 10–19]. They were earlier recognized as anodic inhibitors [2, 4, 9-10] in neutral and alkaline waters and as mixed inhibitors in strong acidic media [20]. Further, molybdates are considered to promote the active–passive state on the surface of steel, which reduces the passivation current through the formation of a stable film and extends the anodic passive range [7, 10, 15, 21]. The inhibition of localized corrosion in CS and aluminum using single, binary and ternary mixtures with molybdates has also been reported [5, 7, 22–27]. Moreover, many previous authors [4, 13, 15-16] have suggested the adsorption of molybdate anions on the oxide film of the surface, which repairs the defects and pores. However, because the disadvantage of molybdate inhibition in low oxygen content solutions is its weak oxidizing power, molybdates require oxidizing agents to increase their performance [1–4, 12–14]. That said, this shortcoming could prove to be an advantage for the inhibition of galvanic corrosion [1].

The synergistic inhibition of molybdates with other oxyanions has also been studied [3, 5- 6, 8, 17, 28-30]. Because Cu and copper alloys are used with CS in the metalworking industry, it would thus be worthwhile evaluating the performance of combinations of oxyanions under galvanic corrosion conditions. Corrosion inhibition in cooling water systems, reverse osmosis water and soft-treated water of low conductivity used for industrial processes often involves metals of distinct nature. The inhibition process, therefore, depends on temperature, the hydrodynamic conditions of the solution, dissolved oxygen (DO) and pH. The correct application of inorganic inhibitors is thus of great importance in the industrial field.

The present work evaluates sodium molybdate alone and that combined with nitrite, phosphate and silicate in order to compare their effectiveness under galvanic conditions. Different temperatures and hydrodynamic conditions for the aqueous solutions for the working electrodes of Cu, CS and the Cu–CS galvanic couple are studied during the inhibition process and their effects compared.

2. EXPERIMENTAL SECTION

2.1 Materials.

Coupons of Cu UNS C10300 and CS UNS G10200 were employed to construct the working electrodes. The galvanic contact between the Cu–CS coupons was created by using a copper wire fit into small holes on one side of each coupon. The electrode was encapsulated in epoxy resin. The final area of the coupled working electrode was 1.2 cm^2. The Cu:CS area ratio was of 2:1. Working electrodes of Cu and CS were also analyzed separately. The final exposed area for each electrode was 1 cm^2. The surfaces were polished using 600-grit SiC paper, washed with distilled water and then acetone-washed and dried according to ASTM G1-03 and ASTM G3-89 standards [31, 32].

2.2 Inhibited solutions.

Soft-treated water for industrial processes (deionized water) of very low conductivity (3 ± 2 μS/cm) was used to prepare the test solution. Analytical grade Na_2MoO_4, and mixtures using a

1.5:1 ratio with $NaNO_2$, Na_2HPO_4 and Na_2SiO_3 were dissolved in the aqueous solution. The electrical conductivity increased to 178 μS/cm in the MoO_4^{2-} solution, 307 μS/cm in the MoO_4^{2-} + NO_2^- solution, 342 μS/cm in the MoO_4^{2-} + HPO_4^{2-} solution and 580 μS/cm in the MoO_4^{2-} + SiO_3^{2-} solution. Cu, CS and the Cu–CS galvanic couple were analyzed by electrochemical impedance spectroscopy (EIS). This technique can be appropriately used in low conductivity media, because the solution resistance (R_s) is a separable quantity and does not interfere with the determination of the polarization resistance (R_{po}) [12, 33].

2.3 Electrochemical test

EIS experiments were carried out with a GAMRY potentiostat PC4-FAS1. The analyses were performed from 10^5 Hz to 0.01 Hz frequency range. The amplitude of the sinusoidal voltage signal was 10mV and scan rate of 10 points per decade. All EIS scans were run in a conventional cell of three-electrode configuration using potentiostatic control. A silver/silver chloride electrode was used as a reference and a high density graphite bar as a counter electrode. All experiments were immersed in the solution 1 hour before the experiments began. The open circuit potential remained stable during EIS measurements. The experiments were carried out in stagnant solution and under stirring provided by a recirculating water system (1200 rpm) at 25 °C and at 77 °C.

2.4 Surface evaluation.

Micrographs of the exposed surface during 24 hours of immersion in the inhibited solutions were obtained by scanning electron microscopy (SEM). Further, the chemical composition surface was analyzed by energy-dispersive X-ray spectroscopy (EDS).

3. RESULTS AND DISCUSSION

3.1 EIS.

The R_{po} values of the different mixtures was calculated by subtracting R_s from the low frequency intercepts with Z' axes. Equivalent circuits were proposed for each inhibitor system in order to describe the electrochemical behavior according to the EIS results. The fit of these equivalent circuits was developed using the Z-View impedance software.

3.2 Molybdate system.

The R_{po} values for EIS applied to Cu, CS and the Cu–CS couple in the system of 200 ppm of MoO_4^{2-} are plotted in Figure 1.

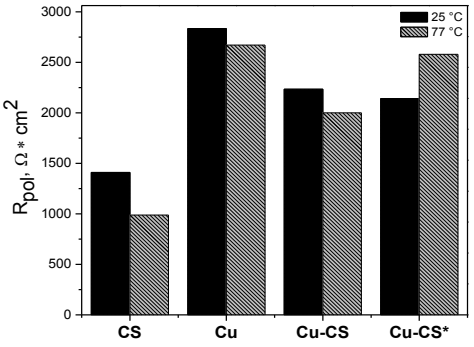

Figure 1. Polarization resistance of CS, Cu, and the Cu–CS couple at 25 °C and at 77 °C in the 200 ppm Na_2MoO_4 solution (stagnant and 1200 rpm circulating rate).

Figure 1 shows the effect of the galvanic conditions on the corrosion inhibition of CS, being the anodic metal of the couple. The MoO_4^{2-} ions have a slightly positive effect on the corrosion inhibition of Cu [10, 15, 17]. As expected, since Cu has a more positive potential than CS [17], the R_{po} of the Cu electrode is greater than that of CS and the Cu–CS couple. CS corrosion resistance improves under the aqueous inhibition of molybdates when CS is coupled with Cu. It has been suggested that galvanic contact promotes Fe^{2+}/Fe^{3+} ion formation [17]. Molybdates thus promote the active–passive transition by interacting with the cations and metal oxide. Many authors have also suggested that MoO_4^{2-} ions are adsorbed on the superficial oxide through the hydrogen bonding of the dangling hydroxyl group of the oxide [8, 17]. However, we find that the R_{po} of the Cu–CS couple is greater than that of CS in the presence of molybdates.

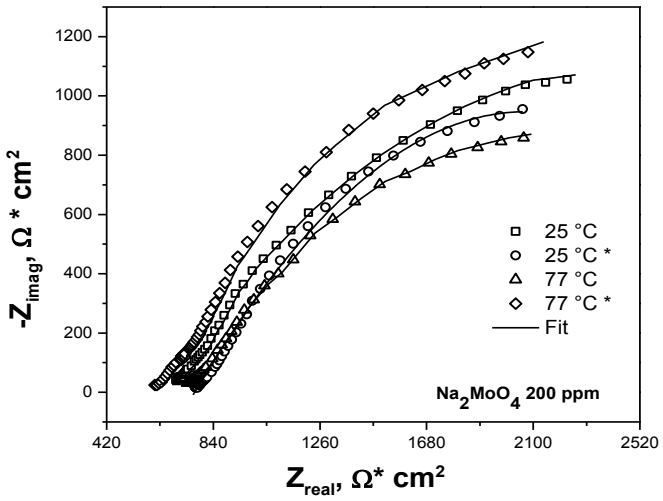

Figure 2. Nyquist plot of the Cu–CS couple at 25 °C and at 77 °C in the 200 ppm Na_2MoO_4 solution (stagnant and 1200 rpm circulating rate).

Therefore, the formation of the iron cations generated by the galvanic effect favors the inhibition process because their interaction with the molybdate forms a protective film. Further, the

inhibition process by molybdates is improved under flow conditions. It has been established that hydrodynamics is a critical factor to control the rate of oxygen transport. At high rotation rates, oxygen transport increases. An initially passive film is formed by the chemisorption of OH^- and O^{2-}, as previously observed on iron in high purity water [34]. The DO is the first passivator of the metal and the molybdate is incorporated later into the passive oxide layer, thus forming the protective compound ferric molybdate [1–9]. The inhibitory properties of molybdates are affected by temperature; however, when the temperature and flow conditions are combined, they promote a synergistic effect that enhances $R_{po.}$

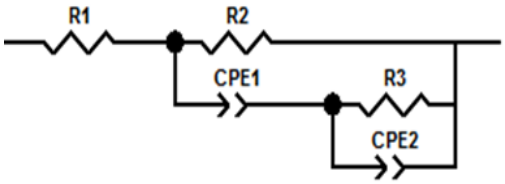

Figure 3. Equivalent circuit proposed for the Cu–CS couple in the Na_2MoO_4 system.

Figure 2 shows the Nyquist plot for galvanic conditions at room temperature and at 77 °C, in stagnant solution and under a flow rate of 1200 rpm. In order to describe the electrochemical behavior of the galvanic couple in the aqueous inhibition of molybdates, an equivalent circuit was proposed (Fig. 3). At high frequency, we observed a slight tendency of points to increase in the direction of Z'' (imaginary component). This shape may occur because of the adsorbed species from the inhibited solutions. A medium frequency semicircle of the great resistance of transfer charge was recorded mainly under flow conditions. This indicates the passive state formed by the protective oxide and the incorporation of MO_4^{2-} that stabilizes the layer through the formation of an insoluble complex. The equivalent circuit proposed for this system suggests a process controlled more by a charge transfer process than by a diffusion process. When the CS surface was coupled with Cu, it presented localized corrosion after 24 hours of exposure at 77 °C (see Fig. 13a). These results suggest searching for a complementary inhibitor in order to increase the performances of molybdate-based corrosion inhibitors.

3.3 Molybdate and nitrite system.

The synergistic effect of $MoO_4^{2-} + NO_2^-$ in neutral and alkaline solutions has already been reported in many works [17, 35–37]. We found that the R_{po} calculated in the 180 ppm MoO_4^{2-} + 120 ppm NO_2^- system is greater than that in the 200 ppm MoO_4^{2-} system (Fig. 4). As suggested earlier, molybdates improve inhibition efficiency in the presence of an oxidizing agent, while corrosion inhibition by nitrite mainly occurs because of its oxidizing property. The ferrous ion produced by galvanic corrosion is converted into an insoluble and stable hydrous ferric oxide that inhibits corrosion in the oxide stability region in near-neutral pH solutions [8]. It is thus expected that during the

inhibition of synergistic corrosion, NO_2^- maintains continuously an oxide layer on the surface and promotes the formation of ferric oxide, especially at defect sites where corrosion takes place. The adsorbed MoO_4^{2-} therefore negatively charges the outer layer and stabilizes the oxide layer, thus avoiding the diffusion of Fe cations [8, 38].

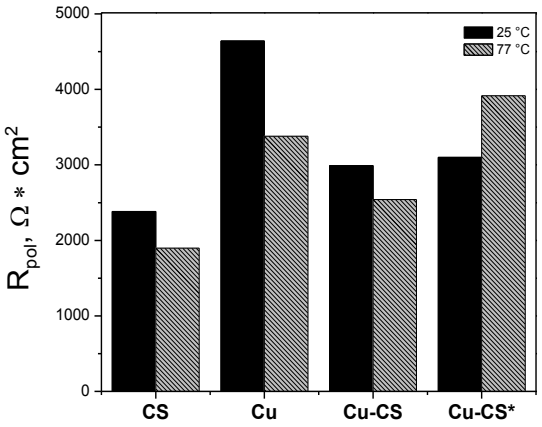

Figure 4. Polarization resistance in CS, Cu, and the Cu–CS couple at 25°C and at 77°C in the Na_2MoO_4 + $NaNO_2$ solution (stagnant and 1200 rpm circulating rate).

The Nyquist plot (Fig. 5) consists of two semicircles: the first semicircle of a small charge transfer at high frequency and the second semicircle at a low frequency followed by the Warburg impedance.

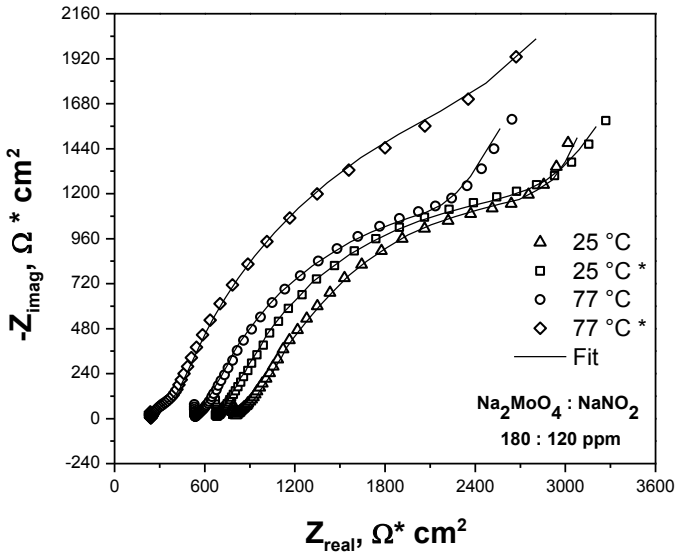

Figure 5. Nyquist plot of the Cu–CS couple at 25 °C and at 77 °C in the Na_2MoO_4 + $NaNO_2$ solution (stagnant and 1200 rpm circulating rate).

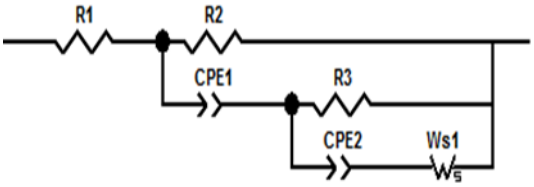

Figure 6. Equivalent circuit proposed for the Cu–CS couple in the Na_2MoO_4 + $NaNO_2$ system.

Table 1. Element values calculated from the impedance measurements of the Cu–CS couple at 25 °C and at 77 °C in the presence of MoO_4^{2-} and NO_2^- (stagnant and 1200 rpm circulating rate).

[Na_2Mo_4] ppm	[$NaNO_2$] ppm	Flow conditions	T °C	R_1 Ω·cm^2	R_2 Ω·cm^2	Y_2, s	R_3 Ω·cm^2	Y_3, s	W s
200	---	stagnant	25	720	480	1.84e-5	2150	1.46e-4	--
			77	675	500	1,91e-5	1983	1.71e-4	--
		flow	25	743	633	1.75e-5	2411	3.11e-5	--
			77	480	633	1.62 e-5	2700	4.87e-5	--
180	120	stagnant	25	508	908	7.45e-6	8341	1.16e-4	0.800
			77	411	1109	2.68e-5	1900	1.36e-4	0.757
		flow	25	552	652	3.79e-6	3200	1.89e-5	0.59
			77	280	458	2.79e-6	4000	1.76e-5	0.57

The equivalent circuit proposed is shown in Figure 6. The fitted calculated values of the impedance plots for 200 ppm of MoO_4^{2-} and 180 ppm MoO_4^{2-} + 120 ppm NO_2^- are described in Table 1. We found that the capacitance values decreased in the presence of MoO_4^{2-} + NO_2^-, which could indicate the great resistance property of the protective layer formed by molybdate–nitrite systems. Unlike the equivalent circuit in the presence of only molybdates (Fig. 3), this equivalent circuit (Fig. 6) considers the Warburg element. The Warburg or diffusional impedance indicates that mass transfer by diffusion controls the electrochemical system. This behavior is because of the diffusion of molybdate and nitrite anions towards the surface electrode in order to protect it. The oxidation of anodic metals using nitrite and DO is recorded by the charge transfer process at a medium frequency (Fig.5). The resistance of the charge transfer at a low frequency semicircle seemed to increase under flow conditions. This step suggests that the oxidation of Fe^{2+} to Fe^{3+} forms ferric molybdate. Further, although R_{po} is affected by temperature, it is enhanced when the system is under active hydrodynamic conditions.

3.4 Molybdate and phosphate system.

Figure 7 shows the R_{po} calculated from the EIS measurements for CS, Cu and the Cu–CS galvanic couple in the presence of the MoO_4^{2-} + HPO_4^{2-} mixture. We found that the Cu electrode

showed the highest R_{po}. The effectiveness of phosphates for inhibiting Cu [39] and that of molybdate–phosphates for inhibiting steel alloys [3] has been well established.

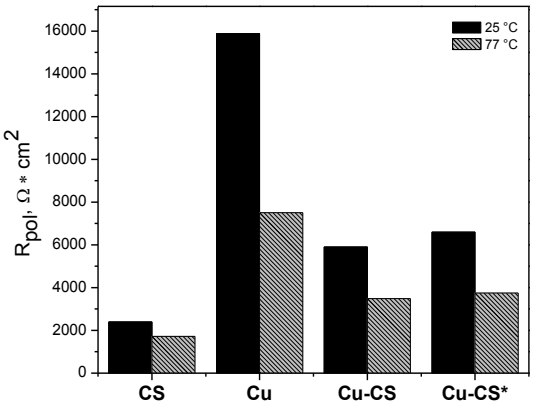

Figure 7. Polarization resistance in CS, Cu, and the Cu–CS couple at 25 °C and at 77 °C in the Na_2MoO_4 + Na_2HPO_4 solution (stagnant and 1200 rpm circulating rate).

Greater R_{po} values were recorded from EIS at room temperature than at 77 °C. This indicated that the MoO_4^{2-} + HPO_4^{2-} system was susceptible to fluctuations in temperature [10]. The galvanic contact also favors CS inhibition. The cations generated from the anodic metal and formed oxides interact with the molybdate and phosphate ions [5, 9]. Moreover, phosphorous could exist in the outer part of the passive film, while molybdenum could exist throughout, albeit to a small degree [5].

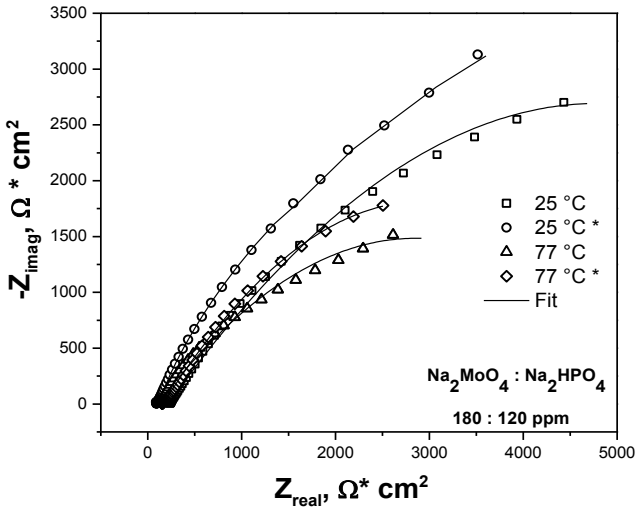

Figure 8. Nyquist plot of the Cu–CS couple at 25 °C and at 77 °C in the Na_2MoO_4 + Na_2HPO_4 solution (stagnant and 1200 rpm circulating rate).

Figure 8 shows the Nyquist plot for the MoO_4 + HPO_4 system. The impedance measurement recorded a charge transfer process of high resistance. The proposed equivalent circuit is shown in Figure 9 and the calculated values are presented in Table 2. The electrochemical behavior acts as a mixed process of mass transfer by charge transfer and diffusion. As expected, the double layer

capacitance value (Table 2) decreases at room temperature. The Warburg element thus represents the diffusion of the phosphate and molybdate species, which are then incorporated into the oxide passive layer.

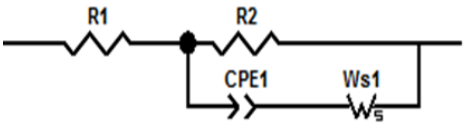

Figure 9. Equivalent circuit proposed for the Cu–CS couple in the Na_2MoO_4 + Na_2HPO_4 and Na_2MoO_4 + Na_2SiO_3 systems.

Phosphates are effective inhibitors in the presence of oxygen [9], because DO oxidizes iron to γ-Fe_2O_3 and the discontinuities in the oxide film are repaired by ferric phosphate. Therefore, the formation of this compound is the main factor that protects steel in phosphate-inhibited solutions [3, 5, 9].

Table 2. Element values calculated from the impedance measurements of the Cu–CS couple at 25 °C and 77 °C in the presence of MoO_4^{2-}, HPO_4^{2-} and SiO_3^{2-} (stagnant and 1200 rpm circulating rate).

[Na_2Mo_4] ppm	[Na_2HPO_4] ppm	[$NaSiO_3$] Ppm	Flow conditions	T °C	R_1 Ω·cm^2	R_2 Ω·cm^2	Y_2, s	n	W s
180	120	---	stagnant	25	351.7	4105	1.84e-5	0.86	0.59
				77	301	6218	1.91e-5	0,87	0.57
			flow	25	297	4423	1.63e-5	0,77	0.69
				77	258	6702	1.78e-5	0,81	0.59
180	---	120	stagnant	25	376	908.9	7.45e-6	0.82	0.55
				77	279	1109	2.68e-5	0.71	0.57
			flow	25	355	18700	1.35e-5	0.77	0.59
				77	280	22863	1.24e-5	0.79	0.56

3.5 Molybdate and silicate system.

The effectiveness of silicate as a corrosion inhibitor for CS has shown a good performance and synergistic features when mixed with other inorganic compounds [20, 40-41]. Indeed, silicates have been used for over 60 years [9]. The R_{po} values showed synergistic behavior with molybdates in the inhibition process (Fig. 10). Even though the silicates were affected by fluctuating temperature [9], the combination of 180 ppm MoO_4^{2-} + 120 ppm SiO_3^{2-} showed high stability and the highest R_{po} values. The inhibition process also improved under flow conditions, as in the other systems.

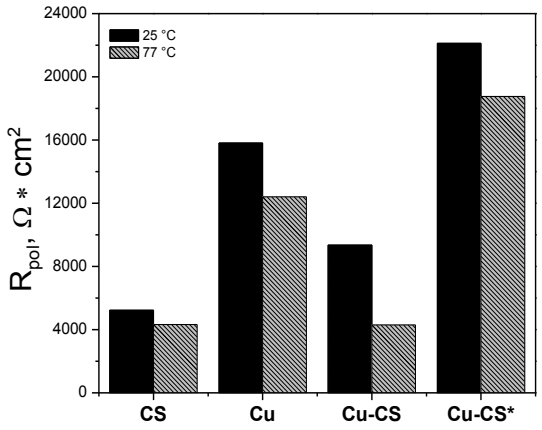

Figure 10. Polarization resistance in CS, Cu, and the Cu–CS couple at 25 °C and at 77 °C in the Na_2MoO_4 + Na_2SiO_3 solution (stagnant and 1200 rpm circulating rate).

Figure 11 shows the Nyquist plot for the Cu–CS galvanic couple in a solution inhibited by the MoO_4^{2-} + SiO_3 mixture. The semicircle represents the high resistance of charge transfer owing to the protective film formed from the hydrated gel of silica [30] and the ferric molybdate. The capacitive behavior is pronounced from high frequencies and recorded an active–passive transition, which thereby offers good protection against galvanic corrosion. Both corrosion inhibitors have been considered to inhibit Cu [27]. The total surface of the galvanic couple is protected under a MoO_4^{2-} + SiO_3^{2-} system. The hydrodynamic conditions improve inhibition performance, as in the previously tested systems. Solution flow promotes the diffusion of the species towards the electrode surface, and thus the passive state is faster and R_{po} increases. The structure of the oxide layer in the presence of the MoO_4^{2-} and SiO_3^{2-} system is Fe_2O_3/FeO/Fe [30]. This layer is stabilized by MoO_4^{2-} and a hydrated gel film of silica.

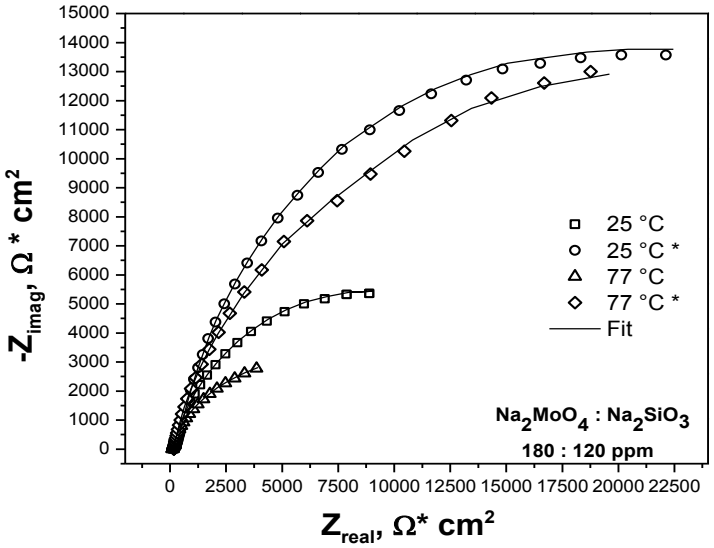

Figure 11. Nyquist plot of the Cu–CS couple at 25 °C and at 77 °C in the Na_2MoO_4 + Na_2SiO_3 solution (stagnant and 1200 rpm circulating rate).

MoO_4^{2-} combined with HPO_4^{2-} or SiO_3^{2-} seems to display a similar electrochemical behavior. The same equivalent circuit was proposed for both systems (Fig. 9). The difference to the NO_2^- combination is the oxidizing power and the fact that the inhibition process changes under galvanic conditions.

3.6 Surface evaluation.

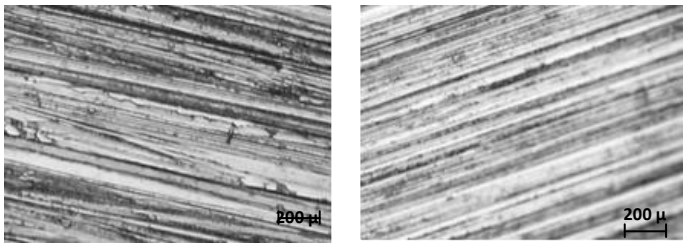

Figure 12. Surface prepared before immersion. **a)** Cu and **b)** CS.

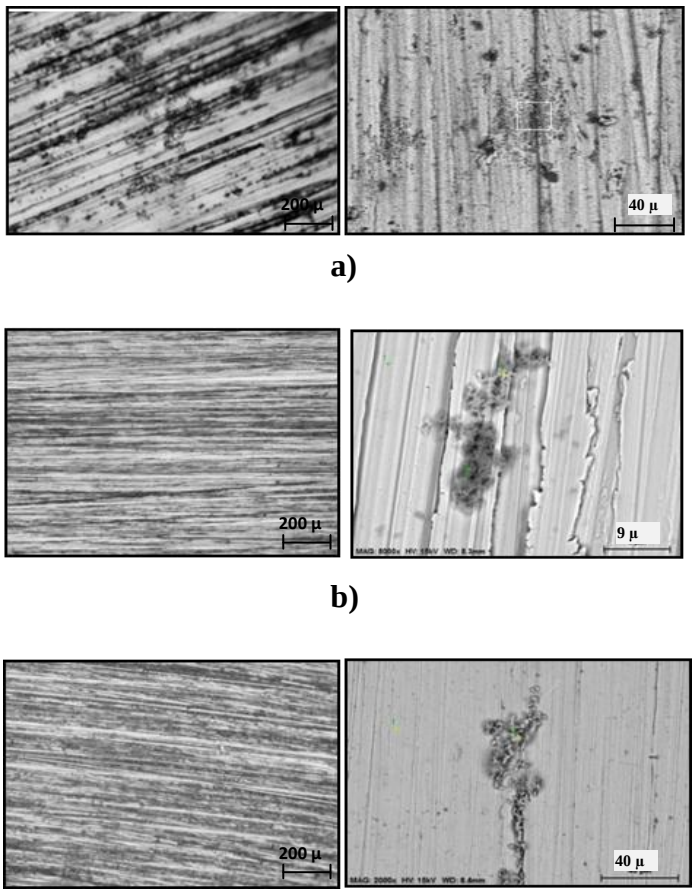

Figure 13. Surface micrograph after exposure **a)** CS coupled with Cu in the 200 ppm molybdate solution at 77 °C**, b)** Cu coupled with CS in 180:120 ppm of the Na_2MoO_4:Na_2SiO_3 solution at 77 °C under flow conditions and **c)** CS coupled with Cu in 180:120 ppm of the Na_2MoO_4 + Na_2SiO_3 solution at 77 °C under flow conditions.

In order to compare the lowest R_{po} recorded (obtained only in the MoO_4^{2-} system) with the highest R_{po} (obtained in the MoO_4^{2-} + SiO_3^{2-} system), the respective surfaces were analyzed by SEM. Figure 12 shows the surfaces before exposure.

The CS surface (Fig. 13a) initially presents surface defects because of localized corrosion promoted by the insufficient inhibition of molybdates at 77 °C. The surface areas presented in Figure 13b for Cu and Figure 13c for CS, magnified by SEM, show the local deposition of the molybdate–silicate combination. Further, the experiments performed by EDS identified traces of Si and Mo in the layer composition (Fig. 14).

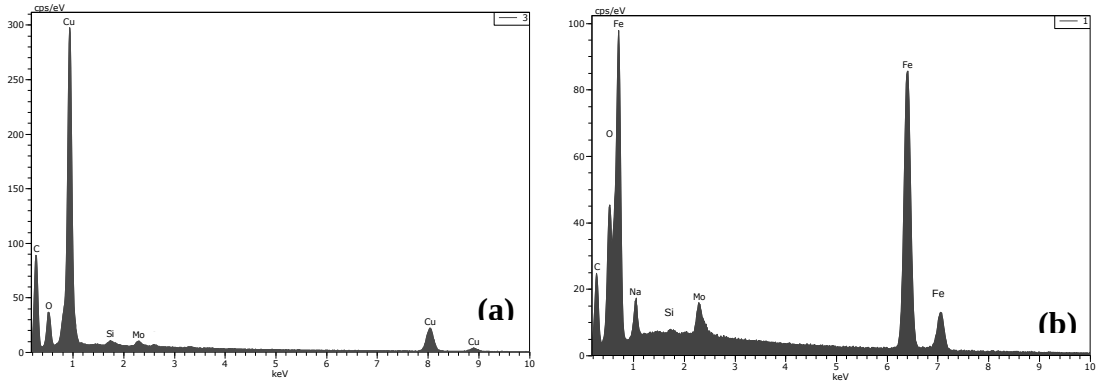

Figure 14. EDS spectrum after exposure **a)** Cu coupled with CS in 180:120 ppm of the Na_2MoO_4 : Na_2SiO_3 solution at 77°C under flow conditions and **b)** CS coupled with Cu in 180:120 ppm of the Na_2MoO_4 + Na_2SiO_3 solution at 77 °C under flow conditions.

3.7 Summary.

Based on the obtained results, we observed the need to combine molybdates with other oxyanions in order to improve performance. Different values of R_{po} were recorded for the metals separately and coupled, thus implying the importance of applying effective inhibitor combinations to protect against galvanic corrosion. The roll of oxygen was of great importance to the four systems presented in this work. In all cases, the flow conditions improved inhibition performance, suggesting that the first passivator is DO. Therefore, the oxyanions are incorporated into the oxide layer with the exception of nitrite. The equivalent circuit proposed for the combination of silicate/phosphate with molybdates differs from molybdates alone and combined with nitrite. When molybdates are alone and under galvanic conditions, a transfer charge process, enhanced by temperature, controls the metal–solution interface and a porous oxide layer is thus formed because of the insufficient inhibition by molybdates at the proposed concentration. A double constant phase element was proposed in the presence of nitrite but with a Warburg element, because the polarization resistance was a combination of diffusional impedance and charge transfer resistance. In the presence of phosphates and silicates, this behavior acts as a capacitor of the great resistance of charge transfer, even when this oxyanion increases the conductivity of the solution. Phosphates and silicates act as passivators, thereby decreasing and stabilizing the anodic current and incorporating it into the oxide film. An advantage of

phosphates and silicates in iron inhibition is the increase in the pH of the solution. The stability of the iron oxide surfaces thus increases with a rise in pH [8]. Molybdate-phosphate system showed high R_{po} when they were applied at Cu alone. Nevertheless, the effectiveness of the molybdates and phosphates combination decreases with the temperature increase under galvanic conditions. Moreover, the molybdate-silicate system showed greater R_{po} values compared with molybdate and nitrite combination. Finally, these results suggested that the molybdate-silicate system was effective to protect Cu, CS and the galvanic couple Cu-CS from corrosion in four different conditions of flow (stagnant and 1200 rpm) and temperature (25 °C and 77 °C). In the industry branch, these data can be apply directly to reduce cost and product manages using the same combination of inhibitors in different hydrodynamic conditions and temperature to protect Cu, CS and inhibit the Cu-CS galvanic corrosion that can be generated within industrial processes.

4. CONCLUSIONS

Three mechanisms for the formation of passive layers during corrosion inhibition were analyzed in this paper using EIS. We showed that the effect of DO, the diffusion process, solubility and the salt dissociation rate combined correctly improves corrosion inhibition. To improve the effectiveness of molybdates as corrosion inhibitors we thus suggest combining them with the correct oxyanion in order to obtain synergistic results of inhibition. Even though temperature affects some systems, the hydrodynamic conditions still improve the corrosion inhibition of the Cu–Cs couple, thus promoting oxygen and the oxyanions towards the electrode surface, reaching the highest R_{po} at 22000 $\Omega \cdot cm^2$ in the presence of molybdates and silicates. Molybdates can be adsorbed by the cations and oxides of the metal in anodic zones through the process of electrostatic attraction. Therefore, the galvanic contact favors the formation of iron ions, which increases the R_{po} of the protective layer.

ACKNOWLEDGMENTS
This research work was carried out thanks to the support of the National Council of Science and Technology (CONACYT) through the scholarship 208739 to Irene Carrillo, intern of this Council.

References

1. W. D. Robertson, *J. Electrochem. Soc.*, 98, (1951), 94
2. M. J. Pryor and M. Cohen, *J. Elctrochem. Soc.*, 100, (1952), 203
3. A. Al-Borno, M. Islam and r. Khraishi, *Corrosion*, 45, (1989), 970
4. A.M. Shams and L. Wang, *Desalination*, 107, (1996), 29
5. H. Yashiro, A. Oyama and K. Tanno, *Corrosion*, 53, (1997), 290
6. D.B. Alexander and A.A. Moccari, *Corrosion*, 49, (1993), 922
7. C. R. Alentejano, I. V. Aoki, *Electrochim acta*, 49, (2004), 2779
8. M.R. Ali, C.M. Mustafa and M. Habib, *J. Sci. Res.*, 1, (2009), 82
9. V.S. Sastri, *Green Corrosion inhibitors*, John Wiley & Son, New Jersey (2011).
10. M.S. Vukasovich and J.P. G. Farr, *Polyhedrom*, 5, (1986), 551

11. M.A Stranick, *Corrosion*, 40, (1984), 296
12. D.G. Kolman and S.R. Taylor, *Corrosion*, 49, (1993), 622
13. R. A. Majed, *Eng. & Tech. Journal*, 27, (2009), 16
14. A.M. Shamms, R.A. Mohamed and H.H. Haggag, *Desalination*, 114, (1997), 85
15. J.P.G. Farr and Saremi, *Surf. Technol.*, 19, (1983), 137
16. M. Saremi, C. Dehghanian, M. Mohammadi Sabet, *Corrs. Sci.*, 48, (2006), 1406
17. C.M Mustafa and S.M. Shahinoor, *Corrosion*, 52, (1996), 16
18. Y. Y. Thangam, M. Kalanithi, C. M. Ambarasi, *Arab. J. Sci. Eng.*, 34, (2009), 49
19. M. Cenoui, N. Dkhireche, O. Kassou, M. Ebn Touhnami, R. Touir, A. Dermaj, N. Hajjaji, *J. Mater. Environ. Sci.*, 1, (2010), 84
20. G. Mu, X. Li, Q. Qu, J. Zhou, *Corrs. Sci.*, 48, (2006), 445
21. K. Aramaki, *Corrosion*, 55, (1999), 1020
22. G. Ruijini and M. B. Ives, *Corrosion*, 45, (1989), 572
23. J. M. Zhao, Y. Zuo, *Corrs. Sci.*, 44, (2002), 2119
24. G.O. Ilevbare, G.T. Burstein, *Corrs. Sci*, 45, (2003), 1545
25. K.C. Emregül, A. A. Aksüt, *Corrs. Sci.*, 45, (2003), 2415
26. V. Moutarlier, S. Pelletier, F. Lallemand, M.P. Gigandet, Z. mekhalif, *Appl. Surf. Sci.*, 252, (2005), 1739
27. V. S. Saji, *Recent Patents on Corrs. Sci*, 2, (2010), 6
28. J.P.G. Farr and M. Saremi, *Surf. Technol.*, 17, (1982) 19
29. T.R Weber, M.A Stranick, M.S. Vukasovich, *Corrosion*, 42, (1986), 542
30. J. R. Chen, H. Y. Chao, Y. L. Lin, I. J. Yang, J. C. Oung and F. M. Pan, *Surf. Sci.*, 247, (1991), 352
31. ASTM G1-03: *Standard practice for preparing, cleaning and evaluating, corrosion test specimens*, ASTM International, 03.02 (1999)
32. ASTM G3-89 : *Standard practice for convention applicable to electrochemical measurements in corrosion testing*, ASTM International, 03.02, (2004)
33. J.R. Scully, D.C. Silverman, M.W. Kendig, *Electrochemical Impedance: Analysis e Interpretation*, ASTM International, Philadelphia (1993)
34. N. Murray, P.J. Moran, E. Gileadi, *Corrosion*, 44, (1988), 533
35. A.A. Al-Refaie, J. Walton, R.A. Cortis and R. Lindsay, *Corrs. Sci.*, 52, (2010), 422
36. I. Carrillo, B. Valdez, R, Zlatev, M. Stoycheva and M. Schorr, *Int. J. Corrs.*, 2011, *(*2011), 1
37. A.A. Al-Refaie, R. A. Cottis and R. Lindsay, *NACE Corrs. conf. and expo.*, Atlanta, Georgia, (2009)
38. J. P. G. Farr A. M. Saremi, A. M. Seeney, A. J. Bentley and L.G. Earwrker, *Polyhedron*, 5, (1986), 547
39. M. M. Antonijevic and B. Petrovic., *Int. J. Electrochem. Sci.*, 3, (2008), 1
40. O. Girciene, R. Ramanauskas, L. Gudavi ˆci and A. Martuŝiene, *Corrosion*, 67, (2011), 125001-1
41. N. Fujita, C. Matsuura and K. Ishigure, *Corrosion*, 45, (1989), 901